



## Supporting Information

for *Adv. Mater. Technol.*, DOI: 10.1002/admt.201800395

### High-Precision Stereolithography of Biomicrofluidic Devices

*Alexandra P. Kuo,\* Nirveek Bhattacharjee, Yuan-Sheng Lee,  
Kurt Castro, Yong Tae Kim, and Albert Folch*

## SUPPLEMENTARY INFORMATION

### Derivation of Cure-Depth versus Exposure Time Relation from Beer-Lambert Law

According to the Beer-Lambert law, the absorbance ( $A$ ) of the resin, which is defined as the logarithmic ratio of the incident intensity ( $I_0$ ) and the intensity of the transmitted light ( $I$ ) is linearly related to the path length traversed by the light through the resin ( $l$ ) and the molar absorptivity ( $\epsilon$ ) and concentration ( $c$ ) of the absorbing species in the resin.

$$(1) \quad A \equiv \log_{10} \left( \frac{I_0}{I} \right) = \epsilon l c$$

The Beer-Lambert law can be rewritten in the exponential form as follows:

$$(2) \quad I(z) = I_0 e^{-2.303 \epsilon c z}$$

where  $I(z)$  is the intensity of the light at a depth  $z$  in the resin.

Let us assume that the exposure time required for the resin at the bottom of the vat (which is closest to the light source) to start curing is  $T_0$ . Since the incident intensity of the light at the bottom of the vat is  $I_0$ , the threshold energy required for curing of the resin ( $E_c$ ) can be written as:

$$(3) \quad E_c = I_0 T_0$$

If  $z_r$  is the depth of the resin that is polymerized (cure-depth) when the total exposure time is  $t_r$ , it follows that the dose of energy at the depth  $z_r$  is equal to the threshold energy of curing,  $E_c$ . Therefore, if  $I(z_r)$  is the intensity of the light at a depth  $z_r$  in the resin, then

$$(4) \quad E_c = I_{z_r} t_r$$

Using  $z = z_r$  in equation (2), and combining equations (3) and (4), we get

$$(5) \quad I_0 T_0 = I_0 e^{-2.303 \epsilon c z_r} t_r$$

Hence, we can show that the cure-depth,  $z_r$ , is linearly related to the logarithm of the exposure time,  $t_r$ , according to the following equation,

$$(6) \quad z_r = h_d \ln \left( \frac{t_r}{T_0} \right)$$

where  $h_d$  is the characteristic penetration depth of the resin defined by

$$(7) \quad h_d = \left( \frac{1}{2.303 \epsilon c} \right)$$

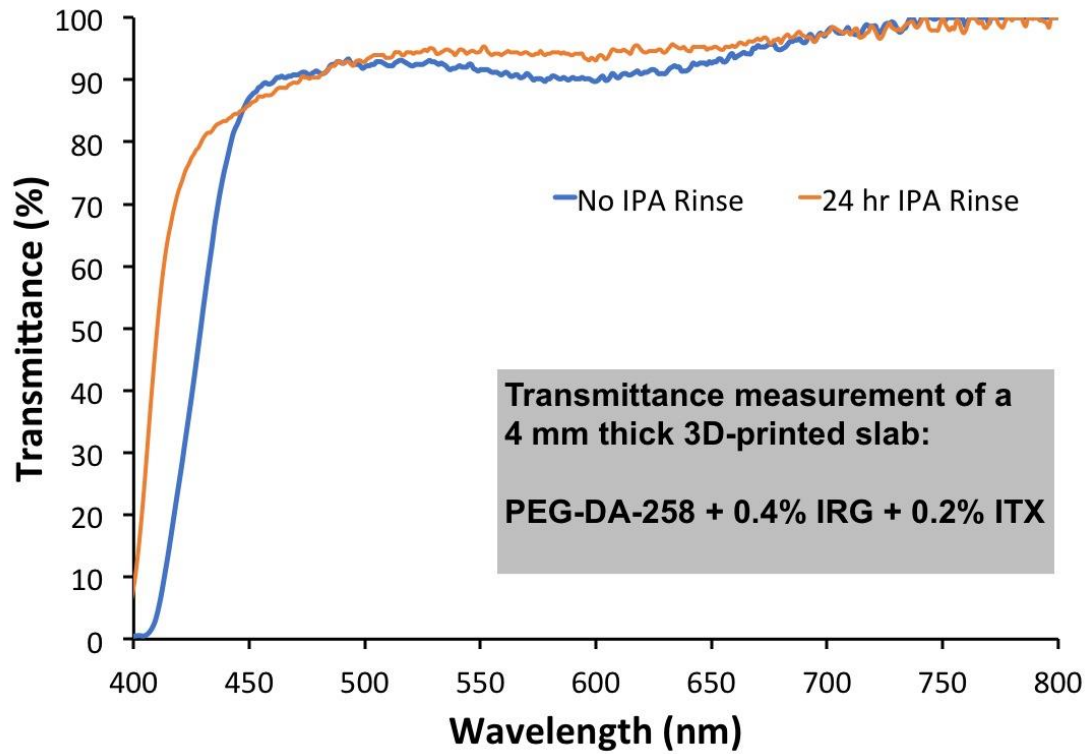
Therefore, the slope of a log-linear plot between  $z_r$  and  $t_r$  will give the characteristic penetration depth of the resin.

### **Pixelation Effects**

We note that the software of some commercial 3D printers (such as the Asiga Pico2 HD) automatically rotate 3D-printed objects at a 45° angle to print lines of pixels cleanly rather than the default diamond configuration of the DMD mirror. If this rotation is not corrected (as has been done in all our prints in this manuscript), the prints can turn out with jagged lines as seen in Figure 2a&d.

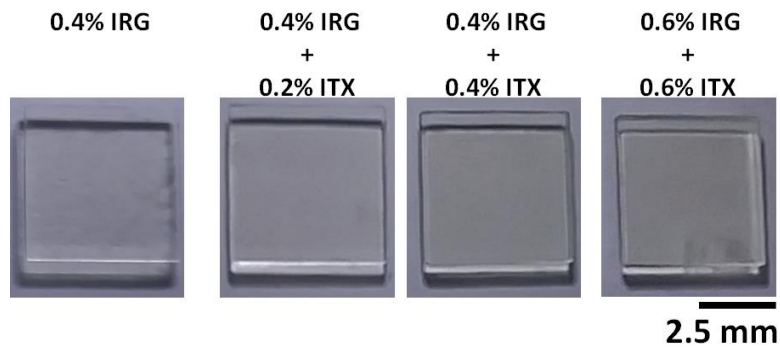
Also, the software used to slice the objects and convert them into an image sequence can result in certain printing inaccuracies where the XY area of a print is not divisible by the pixel size, and thus the software will omit/insert pixels in order to account for the exposure area per slice. This software problem can result in dramatic failures when single-pixel features are printed, where if the print area is not divisible by the pixel size, some single pixels may fail to print in individual slices.

**Supplemental Figure 1:**



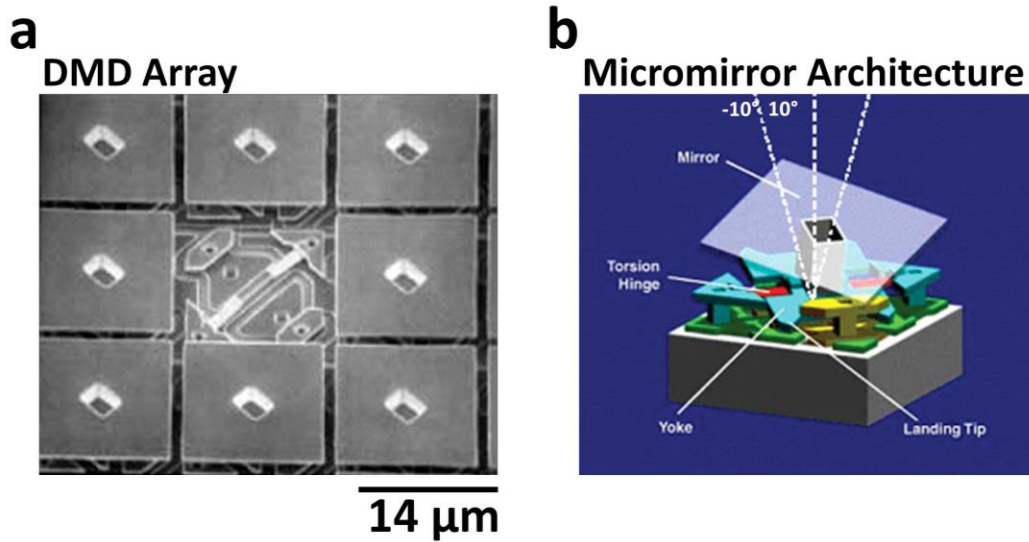
Transmittance curves of 4 mm thick 3D-printed parts of PEG-DA-258 (0.4% IRG and 0.2% ITX) – measurements were taken immediately after printing (blue) and after rinsing in isopropyl alcohol for 24 hours (orange).

**Supplemental Figure 2:**



a) Top view micrographs of 3D-printed 5 mm square blocks, 500  $\mu\text{m}$  thick printed with (0.4% IRG + 0% ITX, 0.4% IRG + 0.2% ITX, 0.4% IRG + 0.4% ITX, 0.6% IRG + 0.6% ITX) from left to right. Slight yellowing pigmentation is noticeable as photosensitizer and photoinitiator amount is increased.

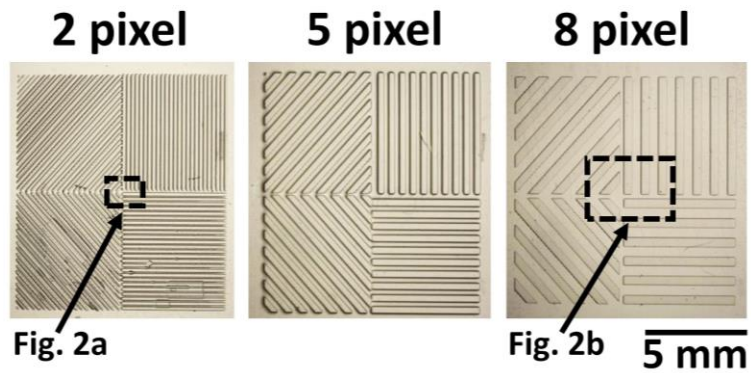
**Supplemental Figure 3:**



a) Commercial 3D printer's UV-LED DLP is based on a Digital Mirror Display (DMD) chip that consists of square-shaped deflectable-micromirrors arranged in a rectangular array with each mirror having a central attachment point and the gaps between mirrors which result in sub-structures in our prints. Figure adapted from [http://www1.cs.columbia.edu/CAVE/projects/pi\\_micro/pics/dmd.jpg](http://www1.cs.columbia.edu/CAVE/projects/pi_micro/pics/dmd.jpg)

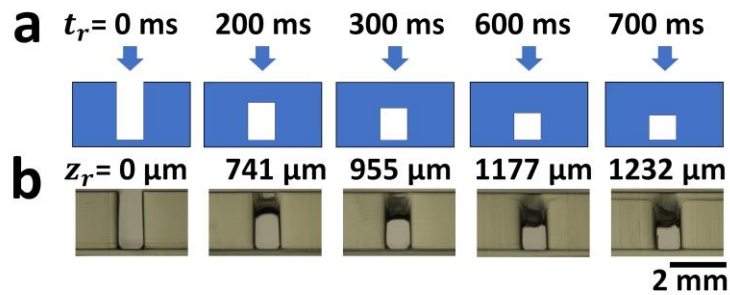
b) Each micromirror is responsible for projecting one pixel of the DLP) as the torsion hinge rotates each mirror for each pixel.

**Supplemental Figure 4:**



3D-printed 2-pixel-wide (left), 5-pixel-wide (middle), and 8-pixel-wide (right) lines at three different orientations (vertical, horizontal and diagonal) that are designed to be 200  $\mu\text{m}$ -high printed with four 50  $\mu\text{m}$  Z-layers using PEG-DA-258 resin containing 0.4% IRG and 0.4% ITX. The dashed boxes are outlined areas of Figure 2a and Figure 2b as labeled.

**Supplemental Figure 5:**



a) Cross-section schematic of the photopolymerization of flat roof layers over a 1 mm-wide, 2 mm-tall gap supported by 200  $\mu\text{m}$ -wide walls. Different times of exposure ( $t_r$ ) will result in roofs of different thicknesses, according to equation 2.

b) Phase-contrast micrographs of the side views of 3D-printed structures printed with 0.4% IRG and 0% ITX PEG-DA-258 resin. The measured thickness of the polymerized roof structures  $z_r$  is displayed above each image corresponding to the different times of exposure  $t_r$  shown in (a).



**Supplemental Video 1:**

Top video of a 3D printed rotary mixer controlled by 6 individually actuated microvalves (Fig. 6d), labeled V1-V6 (Fig. 6e). The individually controlled microvalves allow for rapid mixing (under 1.5 min) of yellow and blue dye by sequentially opening and closing V3, V4, and V5, mixing the fluid in a counterclockwise flow pattern where the control channel pressure was 3 psi for V1 to V5 while for V6 the control channel was 7 psi to prevent leaking to mixed fluid outlet (M1). Valve 6 is closed during mixing and is opened to flow mixed green dye to the M1 by individual control valve actuation (Fig. 6g).